

Deep Learning Based Method for the Estimation of Patient's Angles from Lateral Skull Radiographs

Kazuma NAKAZEKO^{a, b, 1}, Shinya KOJIMA^c, Hiroyuki WATANABE^d and Hiroyuki KUDO^e

^a*Department of Radiological Technology, Faculty of Health Science, Juntendo University, 1-5-32, Yushima, Bunkyo-Ku, Tokyo, Japan*

^b*Graduate School of Systems and Information Engineering, University of Tsukuba, 1-1-1 Tennoudai, Tsukuba, Ibaraki, Japan*

^c*Department of Medical Radiology, Faculty of Medical Technology, Teikyo University, 2-11-1, Kaga, Itabashi-Ku, Tokyo, Japan*

^d*Graduate School of Health Sciences, Showa University, 1865, Tookaichibacho, Midori-ku, Yokohama, Kanagawa, Japan*

^e*Division of Information Engineering, Faculty of Engineering, Information and Systems, University of Tsukuba, 1-1-1 Tennoudai, Tsukuba, Ibaraki, Japan*

Abstract. Radiography is used for initial diagnosis and postoperative follow-up. If a radiograph is deemed unsuitable for diagnosis, it is rejected. Retaking a radiograph is disadvantageous for the patient because it prolongs the examination time and increases the radiation dose. Skull radiography is the position in which retaking occurs most frequently. In skull radiography, the patient's rotational direction is estimated from minute changes in the inner ear's structure in the lateral skull radiograph. When retaking, the amount of correction for patient positioning is generally estimated from the errors in the rejected image through empirical evidence. Therefore, considerable expertise is needed to correct the positioning appropriately, and inexperienced radiologic technologists take considerable time to estimate this error. This study aimed to estimate the patient's angle from lateral skull radiographs to compensate for radiologic technologists' lack of experience and reduce the burden on patients. The radiograph is a simulated 2-D line-integral projection of a 3-D CT image, and we developed an estimation method using deep learning with supervised training. The network is based on a re-scaled ResNet. The patient's angle was estimated in the lateral and superior-inferior directions. We evaluated the accuracy of estimation with the projected images of 256 simulated cases. The estimation errors were $0.48 \pm 0.41^\circ$ and $0.55 \pm 0.50^\circ$ in the lateral and superior-inferior angles, respectively. These findings suggest that a patient's angle can be accurately estimated from a radiograph using deep learning, compensating for the lack of experience and reducing retaking time.

Keywords. Deep learning, Radiography, Patient's angle, Retaking

¹ Corresponding Author: Kazuma Nakazeko, Department of Radiological Technology, Faculty of Health Science, Juntendo University; E-mail: k.nakazeko.tk@juntendo.ac.jp.

1. Introduction

Radiography is used for initial diagnosis and postoperative follow-up. Radiologic

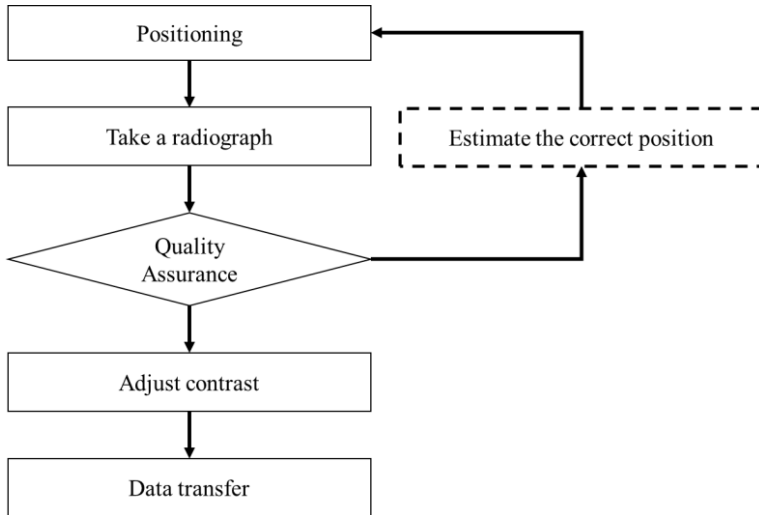


Figure 1. Workflow in taking a radiograph.

technologists must take radiographs suitable for diagnosis. Figure 1 shows the workflow of radiography. First, the radiologic technologist positions the patient and takes a radiograph. Subsequently, they send the contrast-adjusted radiograph to a doctor. However, the doctor might reject it if they find it unacceptable. The major sources of rejection are inappropriate positioning and image quality [1, 2]. The improperly positioned radiograph is not suitable for diagnosis because it cannot clearly show the region to be diagnosed. In addition, a radiograph that contains a lot of noise or has unclear contrast is also not suitable for diagnosis because the region to be diagnosed is unclear. Retaking a radiograph is disadvantageous for the patient because it prolongs the examination time and increases the radiation dose.

The causes of rejection are classified as inappropriate positioning and image quality. Currently, X-ray detectors used in many hospitals use digital radiography (DR). In screen/film systems, the dynamic range is small and does not provide adequate contrast in case of exposure errors (over- and underexposure). DR system has a larger dynamic range than the screen/film system, and adjusting the contrast of the radiograph and correcting it is feasible. Hence, the rejection due to image quality has been reduced. However, the rejection due to positioning is still frequent [3, 4]. The radiographs are positioned so that the diagnosed region overlaps as little as possible with other regions. Skull is composed of many bones and has a complex internal structure. Skull radiography are divided according to the area to be observed. In radiography, which requires observation of detailed areas, a slight deviation in angle makes the radiograph unsuitable for diagnosis. Therefore, skull radiography is the application in which the retaking occurs most frequently [5]. Proper positioning is determined based on the knowledge of anatomy and positioning in radiography. Additionally, experience in evaluating numerous radiographs enables the suitable positioning according to the

patient's physique, which requires appropriate radiographs. The patient's rotational direction needs to be estimated from minute changes in the inner ear's structure in the lateral skull radiograph. When retaking, the amount of correction for the patient positioning is generally estimated from the errors in the rejected image through empirical evidence.

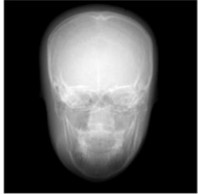
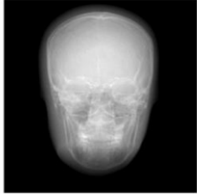
	patient's superior-inferior angle [°]		
	-5	0	5
posteroanterior view			
lateral view			

Figure 2. Differences in images depending on the positioning. Posteroanterior views and lateral views are shown and are compared.

Therefore, considerable expertise is needed to correct the positioning appropriately, and inexperienced radiologic technologists take a long time to estimate this error. This study is aimed at developing a method to estimate the patient's angle from lateral skull radiographs to compensate for radiologists' lack of experience and reduce the burden on patients.

Image processing can be used to estimate the angle of a subject in a photograph. In the field of face recognition, some methods recognize areas of high symmetry, such as faces [6, 7], and some use facial feature points and estimate face angles based on them. On the other hand, in radiography, Seah et al. extracted feature points from a radiograph of the lateral knee joint to estimate tube angles for another positioning [8]. In addition, Wu et al. estimated the rotation angle of the chest from asymmetric projection and validated it using a phantom [9]. However, there exist only two studies that used deep learning to estimate information about the patient's body position from radiographs.

- Ota et al. developed a method to estimate the knee joint rotation direction [10].
- Nakazeko et al. developed a method to estimate the patient's angle from a posteroanterior skull radiograph [11].

We mention that there exist very few previous studies on this topic, because there exist no image processing algorithms for estimating the angles in radiographs, unlike in photographs. A radiograph is a projection image, and feature points are depicted as changes in coordinates if the angle changes. These feature points cannot be represented in conventional image processing algorithms. In contrast, deep learning are powerful

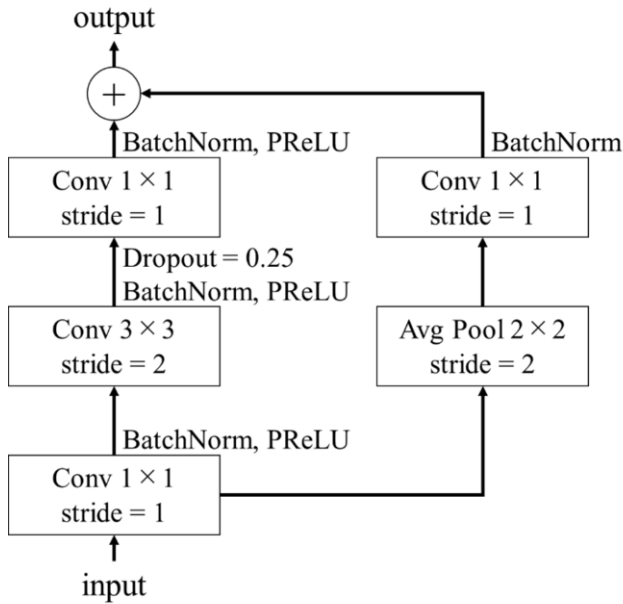


Figure 3. Structure of the residual block.

frameworks which solve the angle estimation problem, in which the mechanism of recognition is unknown, by using training data sets. This study developed a deep learning technique based on a rescaled ResNet (ResNet-RS). We used images of 256 simulated cases to evaluate accuracy of estimating the patient's angles.

Our previous work [11] also studied the problem of estimating the patient's angles from a skull radiograph. The major difference between [11] and this work is as follows. In [11], a radiograph taken from the posteroanterior direction was used. On the other hand, in this work, a radiograph taken from the lateral direction was used. It is known that an image change occurring by the patient rotation is relatively large in the posteroanterior radiograph, but is smaller in the lateral radiograph. Figure 2 compares the posteroanterior and lateral skull radiographs when rotated by $\pm 5^\circ$ in the superior-inferior direction. The posteroanterior skull radiograph shows some discrepancies in the image depending on the rotation direction, as shown in Figure 2. However, the differences in the lateral skull radiographs are not apparent. Therefore, the angle estimation from the lateral one is much more challenging than that from the posteroanterior one. Actually, the method developed in [11] did not work well in the original form for the lateral radiograph case. Therefore, we needed to improve the method in [11] in some parts to obtain successful results in the lateral radiograph case. This improved method is the major contribution of this paper.

2. Proposed Method

We use a deep learning technique to estimate patient angles. This method is based on a ResNet-RS [12]. Figure 3 illustrates the residual block in this model constructed using

Table 1. Architecture of ResNet-RS used.

Name	output size	Layer
stem	128×128	3×3, 64, stride = 2 3×3, 64, stride = 1 3×3, 64, stride = 1
conv 1	64×64	$\left[\begin{array}{l} 1 \times 1, 64, \text{stride} = 1 \\ 3 \times 3, 64, \text{stride} = 2 \\ 1 \times 1, 256, \text{stride} = 1 \end{array} \right] \times 3$
conv 2	32×32	$\left[\begin{array}{l} 1 \times 1, 128, \text{stride} = 1 \\ 3 \times 3, 128, \text{stride} = 2 \\ 1 \times 1, 512, \text{stride} = 1 \end{array} \right] \times 4$
conv 3	16×16	$\left[\begin{array}{l} 1 \times 1, 256, \text{stride} = 1 \\ 3 \times 3, 256, \text{stride} = 2 \\ 1 \times 1, 1024, \text{stride} = 1 \end{array} \right] \times 23$
conv 4	8×8	$\left[\begin{array}{l} 1 \times 1, 512, \text{stride} = 1 \\ 3 \times 3, 512, \text{stride} = 2 \\ 1 \times 1, 2048, \text{stride} = 1 \end{array} \right] \times 3$
C	2×1	Average Pooling, Linear

ResNet-D [13], which is able to suppress overlearning [14] and improve robustness. It uses the PReLU function, which can achieve higher accuracy in image classification [15]. The parameters of the dropout and PReLU functions are determined by trial and error. Table 1 lists the architecture of the network used in this paper. A radiograph is used as the input data; the stem layer downsizes the input data from 256 to 128, and increases the number of channels. Furthermore, the features of radiographs are extracted in convolution layers 1 to 4. Finally, the extracted features are converted into two real numbers representing the angles to be estimated in the last layer. The input data are simulated lateral skull radiographs, and the output data are the real values of the patient's angles in two directions. We explain about the input data in more detail in Section 3.1.1.

The rotation angles are normalized from 0 to 1 by setting the angle at which the patient's median sagittal plane is parallel to the detector to 0° and it takes the range from -10° to 9° in 1° increment. The approximate patient error is in this range, and any further errors can be checked by the radiologic technologist with the sight, so this range was used. The values obtained in the network output and supervised patient's angle are normalized by using the following equation.

$$\text{Normalized value} = \frac{\text{Patient's angle} + 10.0}{20.0} \tag{1}$$

Since the obtained estimated angle is normalized, we convert it into an actual angle by using the following equation,

$$\text{Estimated angle} = \text{Normalized output value} \times 20.0 - 10.0 \tag{2}$$

3. Experiment

3.1. Lateral skull radiograph

A lateral skull radiograph does not show noticeable differences with respect to the patient's rotation compared to a posteroanterior skull radiograph. In the first trial, we tried to estimate the patient's angles using the full lateral skull radiograph as the training

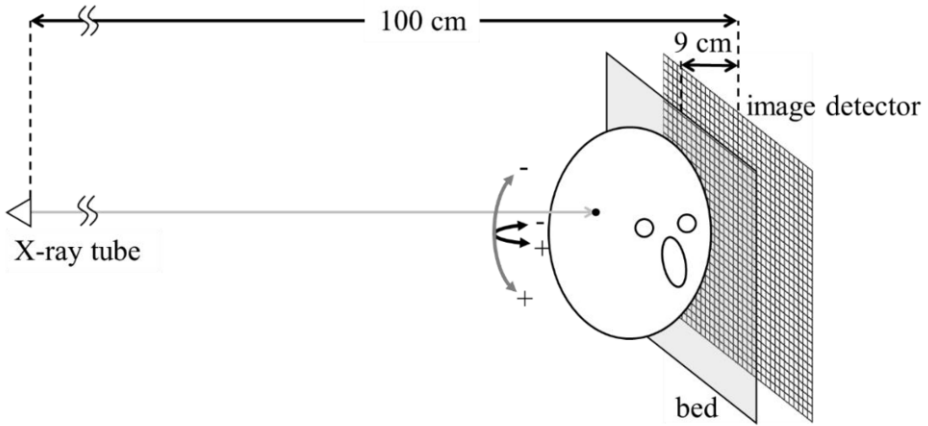


Figure 4. Illustration of simulating skull radiograph.

data. However, the method could not capture minute changes and incorrectly estimated the angles, resulting in a significant error. Since the structure of head is symmetric, the left and right structures overlap in the lateral skull radiograph. Consequently, remarkably similar images can be obtained even when the rotation direction is different. Radiologic technologists empirically estimate the direction of rotation of a symmetrical head based on differences in the magnification of the inner ear structures and temporomandibular joint. The inner ear and temporomandibular joint are located on the left and right sides of the skull, are at different distances from the detector. The differences in magnification make it possible to distinguish the left and right sides on the image. In this study, the estimation is based on the difference in magnification of the inner ear structures. Therefore, an improvement which is able to capture minute changes in the inner ear structure is necessary for accurate estimation. In this study, we propose to use only the region centered on the pituitary gland obtained by a pre-processing image cropping step. The cropping is performed in such a way that the pituitary gland coincides with the center of image, because the center point actually used in the radiograph positioning is approximately the pituitary gland.

3.1.1. Dataset

In our deep learning model, we use an image as the input and two angles as the output. Many image databases are currently available and have been actively used in radiology research. However, no datasets exist which combine the patient's angles with radiographs. Therefore, we constructed an image dataset consisting of simulated

radiographs for this work. Lateral skull radiographs were generated from 3-D CT images through numerical simulation. Figure 4 illustrates the geometric arrangement in skull radiography. In Fig. 4, the hatched and gray rectangular regions represent an image detector and a bed, respectively. A head rotates in the lateral (black arrow) and superior-inferior (gray arrow) direction to simulate a 2-D radiograph image. In the lateral direction, the direction corresponding to the anti-clockwise rotation in the top view was set as positive. In the superior-inferior direction, the direction corresponding to the extension was set as positive. The distances to the x-ray tube and the bed from the detector were 100 and 9 cm, respectively.

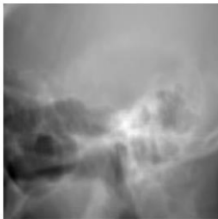
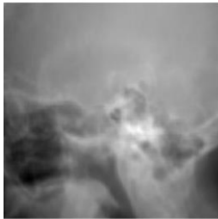
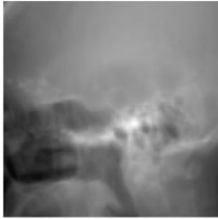
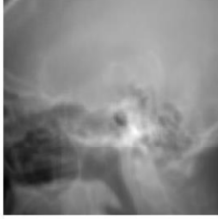
		lateral [°]		
		-10	0	9
superior-inferior [°]	9			
	0			
	-10			

Figure 5. Illustration of simulating skull radiograph.

A lateral skull radiograph is taken with the setup of positioning the patient such that the middle sagittal plane and the detector plane are perpendicular to each other. Then, X-rays are radiated from the perpendicular direction to the detector. A dataset of 3-D CT images after cropping only the head region taken with a PET-CT scanner are provided

in the cancer imaging archive (TCIA) [16]. We used the 3-D CT images in this dataset to construct lateral skull radiographs. We use four different slice thicknesses: 0.6, 1.5, 2.5, and 3.0 mm. The dataset was initially created by setting the rotation angle to 0° in both the lateral and superior-inferior directions. Each radiograph was simulated as a ray-sum images with parallel-beam geometry. For this setting, three radiologic technologists set the angle at which the external auditory meatus overlaps the ray-sum images from multiple directions. Next, the point of X-ray incidence was determined such that the pituitary gland is approximately centered on the ray-sum image. The approximate position of the pituitary gland was used as the X-ray incidence point, because the incidence point is deviated from the radiograph obtained at each position in the clinic. Each radiograph was computed as a simulated 2-D line-integral projection of a 3-D CT image [17]. In more detail, each pixel value in the radiograph was computed by a summation of pixel values of 3-D CT image along the line through which the corresponding X-ray passes, which is expressed as

$$D(x, z) = \sum_{i=1}^N l_i \times p(x_i, y_i, z_i), \quad (3)$$

where $D(x, z)$, N , l_i , and p denote the value of 2-D line-integral projection, the number of pixels such that each X-ray passes, the length of line through each pixel, and pixel value of 3-D CT image, respectively. The matrix size of simulated image was 256×256 (pixels).

As only a portion of the lateral skull radiograph is used in this study, images containing metal artifacts in dental region could also be used. In addition, because changes in the inner ear structure are important features in the angle estimation, we also decided to use CT images without the parietal region. This resulted in the use of images from 256 cases. Figure 5 shows an example of a created lateral skull radiograph. Ota et al. used 60 cases in the previous work, whereas we used 256 cases. Therefore, we used a more significant number of cases in this study than in the existing previous study. Furthermore, in our previous work [11], the number of cases for training data was less than 50 so that we increased the number using a data augmentation, i.e. including images with rotations and images with grid distortion. However, adding the rotated images introduces errors in the relationship between the patient's angle and the simulated radiograph. Furthermore, a portion of the image was extracted in this work to capture minute changes. Using the grid distortion causes errors in the relationship between the minute changes and the patient's angles. Therefore, in this work, training data were used without the data augmentation, because the number of cases was more significant compared to our previous work [11].

3.2. Experimental settings

The construction of the image database was performed using C programming language, but a code to estimate the patient's angle using deep learning was developed using Python. The deep learning was implemented using PyTorch that is an open source machine learning framework on a GPU unit (NVIDIA GeForce RTX 3090). The training of the model was performed by using the Mean Squared Error (MSE) loss function and the Adam optimization method.

The number of training epochs was set to 50, and the weight decay rate was set to 0.00001. The learning rate was changed from 0.0001 to 0.00001 based on the number of iterations, and the batch size was eight, which were determined by trial and error.

3.3. Cross validation

In this study, we used 256 cases. In this 256-case study, 224 cases were used for training and 32 cases for test, i.e. 89,600 images were used for training and 12,800 images for test. These number of images are the number of training and test cases multiplied by 400, since there are 400 images for each case. Cross-validation was performed to validate 256 cases. We divided the 256 cases into eight groups, and performed eight times of testing 32 cases in each group.

Table 2. Summary of estimated error values of lateral and superior-inferior angles. Each value represents the average value of all the 256 cases.

	Average	Standard deviation
lateral	0.48	0.41
superior-inferior	0.55	0.50

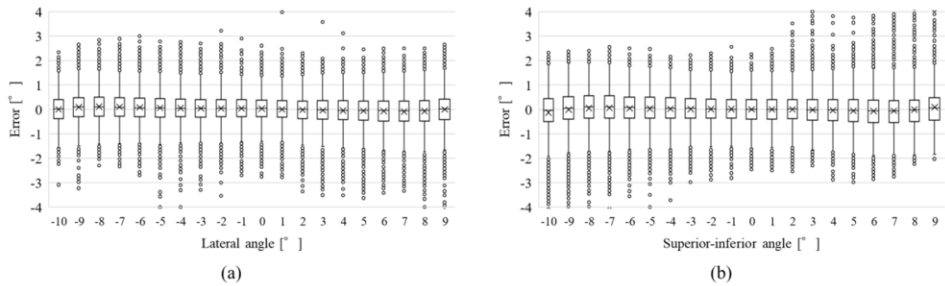


Figure 6. Error values of estimated angles averaged for all the cases.

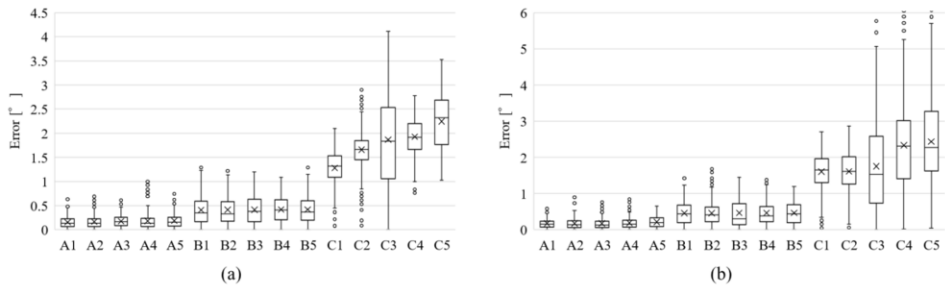


Figure 7. Five typical cases were selected for each group of small (A), medium (B), and large (C) errors.

Hereinafter, we refer to the two estimated patient's angles as “lateral” and “superior-inferior”, respectively.

4. Results

To evaluate accuracy of estimating the patient's angles from the lateral skull radiograph, we used estimation errors for the lateral and superior-inferior angles computed by

$$\text{The estimation error} = \frac{\sum_{i=1}^n |\theta_i - \theta'_i|}{n}, \quad (4)$$

where n , θ , and θ' denote the number of sample cases, the estimated angle, and the

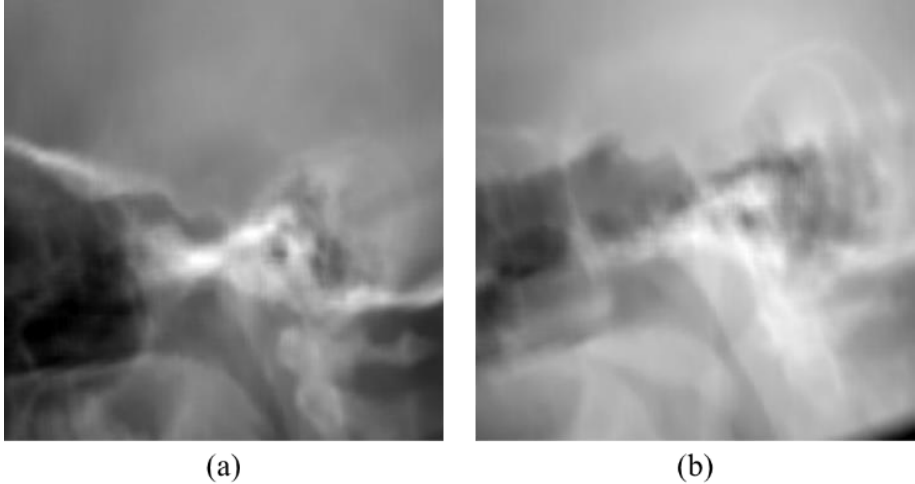


Figure 8. Representative samples with significant estimation error. (a) Case where the contrast between the bone and the other regions is high, (b) case where there was a large shift in the image coordinates.

correct angle, respectively. In Table 2, we summarize average and standard deviation of the errors obtained from all the results of 256 cases. Figure 6 illustrates the estimation errors for the lateral and superior-inferior angles in the corresponding directions. Figure 7 illustrates the estimation errors for each case. In Figs. 6 and 7, each graph shows the distribution of errors into quartiles. Boxes are drawn between the first and third quartiles. Lines in the box show the median value. Solid lines indicate the distribution outside the upper and lower quartiles, and any point outside those lines is considered an outlier. Cross marks and circle marks show the averages and outliers, respectively. Throughout the results, the most significant error found was $2.24 \pm 0.55^\circ$ in the lateral direction and $2.44 \pm 1.32^\circ$ in the superior-inferior direction.

5. Discussion

This work developed a method to estimate the patient's angles using a lateral skull radiograph. Before this development, we constructed an image dataset because no valid datasets with the annotation of patient angles were available in the existing open data. Table 2 summarizes the result of estimation for all the 256 cases. We believe that these results are promising in the following sense. The estimation results for each angle shown in Figure 6 are comparable to those in our previous work [11], in spite of the fact that the estimation from the lateral radiograph is more difficult compared to the

estimation from the posteroanterior radiograph. However, there was a change in error bias (increase or decrease) depending on the angle. This may be because more cases were used in the study than in the previous work.

Figure 8 shows two typical examples of cases with significant errors. Two factors are major sources of these large estimation errors. First, the image contrast in some images was higher than that in the other cases. In the case shown in Figure 8(a), the signal in the bone region is higher than that in the other cases, and the contrast between the bone and the other areas is also high. We suppose that this prevents capturing minute changes in the image due to changes in the angle, leading to a significant error. And, we believe that these errors can be reduced by adding a histogram equalization process to equalize the contrast as a process prior to estimating the angle. The second example is the case where the error becomes large due to the shift of X-ray incident point. In the case shown in Figure 8(b), the incident point is lower than that in the other cases, and there is a coordinate shift in the image. This leads to significant error because the image differs from the other cases. In this case, when the angle was estimated with the correct angle of incidence, the error decreased from $1.86 \pm 1.02^\circ$ to $0.91 \pm 0.58^\circ$ in the lateral direction and from $2.33 \pm 1.32^\circ$ to $0.95 \pm 0.78^\circ$ in the superior-inferior direction. To overcome these drawbacks, the following methods need to be developed to eliminate the factors that increase errors. First, it is necessary to develop a method that can handle various cases by increasing the number of cases. Second, the learning dataset is classified according to the characteristics of each image in the learning step. Then, the model training is performed dependent on each class. In the test step, a model which best matches the input image is selected to obtain output. A method that performs a classification as a pre-processing step enables the construction of such a method. Second, the first error factor will be reduced by developing a method that performs image processing to compensate for variations in image contrast. In addition, it is necessary to develop a pre-processing method that automatically extracts the area centered on the pituitary gland for clinical use. In addition, it is necessary to confirm that the data set is suitable for validation on a clinical device. It is essential to check the relationship between angular errors and image changes that occur when imaging with clinical equipment.

6. Conclusion

We developed a deep learning based method to estimate a patient's angles from a lateral skull radiograph. The estimation results were reasonable, with approximately 0.5° error in both the lateral and superior-inferior directions. Although the estimation from the lateral radiograph is more difficult compared to the estimation from the posteroanterior radiograph dealt in our previous work [11], the accuracy of estimation in this work (lateral) was comparable to that reported in [11] (posteroanterior). This may be thanks to using a significant number of cases in the training. However, there were cases where a considerable error occurred because of differences in the image contrast and the translation in the image coordinates. It is expected that this drawback will be resolved in the future by increasing the number of cases used for training and by using multiple models depending on the image characteristics. In addition, validating the proposed method with images taken from an actual clinical equipment is also an important future work.

7. Acknowledgements

We thank Editage (www.editage.com) for the English language editing.

References

- [1] Kjelle E, Schanche AK, Hafskjold L. To keep or reject, that is the question - A survey on radiologists and radiographers' assessments of plain radiography images. *Radiography (Lond)*. 2021 Feb;27(1):115-119. doi: 10.1016/j.radi.2020.06.020.
- [2] Atkinson S, Neep M, Starkey D. Reject rate analysis in digital radiography: an Australian emergency imaging department case study. *J Med Radiat Sci*. 2020 Mar;67(1):72-79. doi: 10.1002/jmrs.343.
- [3] Kjelle E, Chilanga C. The assessment of image quality and diagnostic value in X-ray images: a survey on radiographers' reasons for rejecting images. *Insights Imaging*. 2022 Mar 4;13(1):36. doi: 10.1186/s13244-022-01169-9.
- [4] Waaler D, Hofmann B. Image rejects/retakes--radiographic challenges. *Radiat Prot Dosimetry*. 2010 Apr-May;139(1-3):375-9. doi: 10.1093/rpd/ncq032.
- [5] Lin C-S, Chan P-C, Huang K-H, Lu C-F, Chen Y-F, Lin Chen Y-O. Guidelines for reducing image retakes of general digital radiography. *Advances in Mechanical Engineering*. 2016;8(4). doi:10.1177/1687814016644127.
- [6] Murphy-Chutorian E, Trivedi MM. Head pose estimation in computer vision: a survey. *IEEE Trans Pattern Anal Mach Intell*. 2009 Apr;31(4):607-26. doi: 10.1109/TPAMI.2008.106.
- [7] Borghi G, Fabbri M, Vezzani R, Calderara S, Cucchiara R. Face-from-Depth for Head Pose Estimation on Depth Images. *IEEE Trans Pattern Anal Mach Intell*. 2020 Mar;42(3):596-609. doi: 10.1109/TPAMI.2018.2885472.
- [8] Seah LJY, Seow D, Mahmood D, Chua EC, Sng LH. Can the measured angle ABC on the lateral projection of the knee be used to determine the tube angulation for an optimum skyline projection? *Radiography (Lond)*. 2022 May;28(2):407-411. doi: 10.1016/j.radi.2021.11.005.
- [9] Wu Z, Hou P, Li W, Zhu T, Wang P, Yuan M, Sun J. Estimating rotation angle from asymmetric projection of chest. *J Xray Sci Technol*. 2021;29(6):1139-1147. doi: 10.3233/XST-210990.
- [10] Ohta Y, Matsuzawa H, Yamamoto K, Enchi Y, Kobayashi T, Ishida T. Development of retake support system for lateral knee radiographs by using deep convolutional neural network. *Radiography (Lond)*. 2021 Nov;27(4):1110-1117. doi: 10.1016/j.radi.2021.05.002.
- [11] Nakazeko K, Kojima S, Watanabe H, Kudo H. Estimation of patient's angle from skull radiographs using deep learning. *J Xray Sci Technol*. 2022;30(5):1033-1045. doi: 10.3233/XST-221200.
- [12] Bello I, Fedus W, Du Xianzhi, Cubuk ED, Srinivas A, Lin T-Y, Shiens J, Zoph B. Revisiting ResNets: Improved Training and Scaling Strategies. *arXiv [Preprint]* arXiv:2103.07579. 10.48550/arXiv.2103.07579
- [13] He T, Zhang Z, Zhang H, Zhang Z, Xie J, Li M. Bag of tricks for image classification with convolutional neural networks. in: Lisa O'Conner, editor. *Proceedings of the IEEE conference on computer vision and pattern recognition*; 2019 June 16-17; Long Beach, CA. USA: Conference Publishing Services; pp.558-67. doi:10.48550/arXiv.1812.01187.
- [14] He K, Zhang X, Ren S and Sun J, Delving deep into rectifiers: Surpassing human-level performance on ImageNet classification. in: Lisa O'Conner, editor. *2015 IEEE international conference on computer vision*; 2015 Dec 7-13; Santiago, Chile: Conference Publishing Services; pp.1026-1034. doi: 10.1109/ICCV.2015.123.
- [15] Hinton GE, Srivastava N, Krizhevsky A, Sutskever I, Salakhutdinov RR. Improving neural networks by preventing co-adaptation of feature detectors. *ArXiv [preprint]*. arXiv: 1207.0580 doi:10.48550/arXiv.1207.0580.
- [16] Clark K, Vendt B, Smith K, Freymann J, Kirby J, Koppel P, Moore S, Phillips S, Maffitt D, Pringle M, Tarbox L, Prior F. The Cancer Imaging Archive (TCIA): maintaining and operating a public information repository. *J Digit Imaging*. 2013 Dec;26(6):1045-57. doi: 10.1007/s10278-013-9622-7.
- [17] Nakazeko K, Kajiwara H, Watanabe H, Kuwayama J, Karube S, Araki M, Hashimoto T, Shinohara H. [Development of computer assisted learning program using cone beam projection for head radiography]. *Igaku Butsuri*. 2012;32(1):2-11. Japanese. doi:10.11323/jjimp.32.1_2.